agriculture

MDPI

Article

Sulfate Nutrition Modulates the Oxidative Response against Short-Term Al^{3+}-Toxicity Stress in *Lolium perenne cv. Jumbo* Shoot Tissues

Hernan Vera-Villalobos [1], Lizzeth Lunario-Delgado [2], Anita S. Gálvez [3], Domingo Román-Silva [4,†], Ana Mercado-Seguel [5] and Cristián Wulff-Zottele [3,*]

1 Centro de Bioinnovación Antofagasta (CBIA), Facultad de Ciencias del Mar y Recursos Biológicos, Universidad de Antofagasta, Antofagasta 1240000, Chile; hernan.vera@uantof.cl
2 Programa de Magister en Biotecnología, Departamento de Biotecnología, Facultad de Ciencias del Mar y Recursos Biológicos, Universidad de Antofagasta, Antofagasta 1240000, Chile; danitza.lunario@gmail.com
3 Departamento Biomédico, Facultad de Ciencias de la Salud, Universidad de Antofagasta, Antofagasta 1240000, Chile; anita.galvez@uantof.cl
4 Departamento de Química, Universidad de Antofagasta, Antofagasta 1240000, Chile
5 Departamento de Biotecnología, Universidad de Antofagasta, Antofagasta 1240000, Chile; ana.mercado@uantof.cl
* Correspondence: cristian.wulff.z@uantof.cl; Tel.: +56-55-2637995
† Dr. Domingo Román-Silva has pass away (Dead).

Abstract: Al^{3+}-toxicity in acidic soils is among the main abiotic stress factors that generate adverse effects in plant growth; in leaves, it affects several physiological parameters such as photosynthesis and ROS balance, leading to limited crop production. On the other hand, sulfur is a macronutrient that has a key role against oxidative stress and improves plant growth in acidic soils; however, the implication of sulfate nutritional status in the modulation of short-term Al^{3+}-toxicity tolerance mechanisms in plant leaves are barely reported. This study is focused on the role of sulfate on the leaf response of an Al^{3}-sensitive perennial ryegrass (*Lolium perenne cv. Jumbo*) after 48 h of exposure. *Lolium perenne cv. Jumbo* seeds were cultivated in hydroponic conditions with modified Taylor Foy solutions supplemented with 120, 240, and 360 µM sulfate in the presence or absence of Al^{3+}-toxicity. The *L. perenne cv. Jumbo* leaves were collected after 48 h of Al^{3+}-toxicity exposure and processed to evaluate the effects of sulfate on Al^{3+} toxicity, measuring total proteins, mineral uptake, photosynthesis modulation, and ROS defense mechanism activation. The plants exposed to Al^{3+}-toxicity and cultivated with a 240 µM sulfate amendment showed a recovery of total proteins and Ca^{2+} and Mg^{2+} concentration levels and a reduction in TBARS, along with no changes in the chlorophyll A/B ratio, gene expression of proteins related to photosynthesis (Rubisco, ChlAbp, and Fered), or ROS defense mechanism (SOD, APX, GR, and CAT) as compared with their respective controls and the other sulfate conditions (120 and 360 µM). The present study demonstrates that adequate sulfate amendments have a key role in regulating the physiological response against the stress caused by Al^{3+} toxicity.

Keywords: aluminum; Al^{3+}-toxicity; sulfate; oxidative stress; antioxidant response

Citation: Vera-Villalobos, H.; Lunario-Delgado, L.; Gálvez, A.S.; Román-Silva, D.; Mercado-Seguel, A.; Wulff-Zottele, C. Sulfate Nutrition Modulates the Oxidative Response against Short-Term Al^{3+}-Toxicity Stress in *Lolium perenne cv. Jumbo* Shoot Tissues. *Agriculture* **2024**, *14*, 1506. https://doi.org/10.3390/agriculture14091506

Academic Editors: Lidija Begović, Ivna Štolfa Čamagajeva, Selma Mlinarić and Yinbo Gan

Received: 13 November 2023
Revised: 30 December 2023
Accepted: 31 December 2023
Published: 2 September 2024

1. Introduction

Soil acidification is the second strongest environmental factor, after desertification, that affects food production worldwide. Acid soils occupy approximately 40% of the total area available for agricultural activity worldwide and 70% of potential lands for agriculture [1,2]. In Chile, the agricultural industry is mostly located in the southern region of the country, where 60% of agricultural lands are taxonomically classified as andosols [3,4], which are characterized by low pH ranges (lower than 5.5) that facilitate the presence of the

toxic aluminum specie of trivalent aluminum (Al^{3+}), which is capable of reducing forage production [3,5].

In this context, Al^{3+}-toxicity's most significant effects on root tissue are cell morphology modifications, leading to poor development of the root apex and the inhibition of root hair development [6]. This damage was observed in Al-sensitive plants as early as 30 min after exposure [7–9], showing that Al^{3+} internalization is a rapid event that occurs mainly by an apoplastic translocation mechanism in plants treated with 1.45 µM Al^{3+} between 30 min and 72 h [10], resulting in negative effects on several cellular pathways such as root cell division, cell wall arrangement, and ROS-induced membrane damage [11–15]. Increased ROS production, an Al^{3+}-toxicity consequence, activates biochemical and physiological mechanisms that prevent oxidative stress, such as gene expression of enzymes involved in ROS catabolism, such as catalase (CAT), glutathione peroxidase (GR), and superoxide dismutase (SOD), along with other enzymes associated with the Halliwell–Asada–Foyer cycle. Consequently, increased ROS catabolism generates an imbalance in the antioxidant metabolites associated with free radical damage reduction, such as ascorbic acid and glutathione [12,16–20]. As mentioned above, Al^{3+}-toxicity affect plant root growth as the first organ directly exposed to this metal toxicity. Consequently, aluminum is transported to leaves through the xylem, affecting the photochemical efficiency of photosystem II and pigment concentration [20]. Studies on varieties of citrus species have shown that Al^{3+} toxicity decreases CO_2 assimilation, stomatal conductance, and soluble proteins, resulting in damage to the light-dependent and -independent phases of photosynthesis [21–23]. In addition, Al^{3+} toxicity was able to modify the activity of enzymes related to ROS defense [24].

To handle Al^{3+} toxicity in agronomy field crops, the addition of alkaline amendments of gypsum ($CaSO_4$) (2.0 ton ha^{-1}) and lime ($CaCO_3$) (7.5 ton ha^{-1})) are used to decrease soil acidity, improving the crop yield of perennial ryegrass, corn and alfalfa by around 30 to 50% [25–27], showing reduced effects of Al^{3+} toxicity in root tissue and improving soil nutrient uptake and plant growth [28,29]. In this context, Kinraide et al., 1991 [30] and Mora et al., 2002 [31] suggested that a gypsum supply ($CaSO_4$ 10/1 sulfate–aluminum ratio) reduced the Al^{3+} toxicity symptoms of andosol-cultivated ryegrass, indicating that $AlSO_4^+$ complexes constitute an important mechanism of Al^{3+} detoxification for this forage species. However, sulfate supply did not reduce the amount of free Al^{3+} available in nutrient solutions, suggesting that $AlSO_4^+$ formation do not play an important role in decreasing Al^{3+}-toxicity in perennial ryegrass roots at short term periods, and further proposes that an adequate sulfate-supply may protect from Al^{3+}-toxicity by adjusting key root homeostatic mechanisms [32]. Additionally, sulfur is an essential macronutrient mainly assimilated by root plants from soil and in a lower degree as SO_2 from the atmosphere by leaves [33] and is used in the synthesis of a variety of molecules, such as amino acids (i.e., cysteine and methionine), antioxidant metabolites (glutathione), phytochelatins, vitamins, and cofactors [34]. This explains the importance of maintaining adequate sulfate nutrition levels to activate the mechanisms involved in sulfate amendment to prevent Al^{3+}-toxicity damage. Recent studies reported that increased sulfate availability enhances physiological and biochemical mechanisms to reduce the effects of long-term Al^{3+}-toxicity, such as a decrease in the lipid damage of biological membranes in *L. perenne cv. Jumbo* roots [18] and Citrus grandis seedlings [24]. On the other hand, Zhu et al., 2018 [35] showed that 2 µM hydrogen sulfide can ameliorate Al^{3+} toxicity in rice roots. Nevertheless, Alarcón-Poblete et al., 2018 [36] reported a scarcity of studies related to the interaction between Al^{3+}-toxicity and sulfur nutrition as well as the molecular approaches involved in Al^{3+} tolerance through sulfate homeostasis. In this context, our previous studies on long-term Al^{3+}-toxicity demonstrated that proper sulfate conditions could improve the plant growth of *L. perenne cv. Jumbo* cultured with four different conditions of sulfate amendments in the presence or absence of aluminum for 28 days [18]. On the other hand, we also demonstrated that Al^{3+} incorporation in *L. perenne cv. Jumbo* roots is a rapid event that causes a disturbance in magnesium and calcium assimilation and activates ROS antioxidant

machinery such as SOD enzymes as early as 48 h after first exposure to Al species in a response modulated by sulfate amendments [32]. Nevertheless, few reports regarding the mechanism of sulfate in modulating short-term (48 h) Al^{3+}-toxicity response in plant leaves are documented.

The present study is the first to describe how sulfate nutrition modulates the response that activates different mechanisms against short-term Al^{3+}-toxicity in Al-sensitive *Lolium perenne cv. Jumbo* leaves. This response includes changes in mineral uptake, photosynthetic parameters, and ROS response in leaf tissue after 48 h of Al^{3+}-toxicity exposure.

2. Material and Methods

2.1. Experimental Growth Conditions and Plant Leaves Tissue Collection

The current study focused on the Al^{3+}-toxicity short-term response in *L. perenne cv. Jumbo* cultivar, an Al-sensitive variety, since it provides a significant response to Al^{3+}-toxicity, and therefore the response activated by sulfate amendment could be observed. Al-sensitive *Lolium perenne cv. Jumbo* seeds were sterilized in 4% sodium hypochlorite (NaClO) solution for 10 min and then washed with distilled water 3 times, as previously described by Cartes et al., 2012 [12]. Then, 50 sterilized seeds were placed in 36 plastic plates (3.5 L pots) each, and were germinated using distilled water under the following controlled conditions: 23 °C and 100 µmol photons m^{-2} seg^{-1} and 60% relative humidity at the Universidad de Antofagasta greenhouse. After 10 days, germinated seeds from 12 plastic plates were transferred into 3.5 L pots filled with aerated Taylor Foy (TF) hydroponic nutrient solution with 120 µM sulfate supply [37]; the remaining 24 plates were transferred to plastic pots filled with modified TF solutions with 240 and 360 µM sulfate supply, and the plants were allowed to grow for 21 days. The detailed nutrient composition of the 240 and 360 µM sulfate hydroponic solutions were described by Vera-Villalobos et al., 2020 [32]. The *L. perenne cv. Jumbo* plants were evaluated in an experimental design with three sulfate conditions (120, 240 and 360 µM) in the presence or absence of 100 µM of $AlCl_3$, according to the protocol described by Vera-Villalobos et al., 2020 [32]. The average concentration of Al^{3+} free metal in 100 µM $AlCl_3$-containing TF nutrient solutions at pH 4.5 was estimated in 8.4 ± 0.1 µM using Geochem-EZ software [38]. The modified TF and increased sulfate supply hydroponic solutions are specified in in the multimedia componenent of the appendix of supplementary data annexed to Vera-Villalobos et al. (2020). The *L. perenne cv. Jumbo* shoot tissues were collected 48 h after the addition of $AlCl_3$. For biochemical and molecular analyses, the plant leaves were frozen in liquid nitrogen and stored at −80 °C until use. On the other hand, to estimate Al, Ca, Mg, and S concentration, the plant leaves were stored in paper bags and dried in an oven at 60° C. The dried plant leaves were weighted for dry mass phenotype analysis and stored at RT until use.

2.2. Aluminum, Calcium, and Magnesium Estimation in Plant Leaves via Atomic Absorption Spectroscopy (AAS)

A total of 150 mg of dried plant leaves previously stored in paper bags was chemically digested as described by Vera-Villalobos et al., 2020 [32]. After digestion, the samples were filtered and analyzed using an atomic absorption spectrometer (ContrAA 300, Analytik Jena, Jena, Germany) based on the work of Román-Silva et al., 2003 [39]. The amounts of Al, Ca, and Mg were normalized to the dry weight of plant leaves in every experimental treatment.

2.3. Sulfur Estimation in L. perenne Leaves via Gravimetry

To obtain the sulfur concentration in plant leaves of *L. perenne cv. Jumbo* subjected to Al^{3+}-toxicity, and their respective controls, in the presence of different sulfate amendments, the gravimetric method described by Vera-Villalobos et al., 2020 [32] was used. Firstly, 5 mL of leaves digested using a microwave oven was transferred to a 10 mL glass beaker. After digestion, 10 mL of $BaCl_2$ solution (HCl 5 M and $BaCl_2$ 5% *w*/*v*) was added and the samples were incubated for 24 h for $BaSO_4$ formation. Then, the samples were filtered through a 0.45 µm pore diameter using Whatman paper and heated at 80 °C to discard any

water traces. Finally, to estimate sulfur concentration, the crystalized $BaSO_4$ was weighted, and the sulfur was calculated.

2.4. Lipid Peroxidation Measurements

Thiobarbituric reactive species (TBARS) were assessed to determine membrane lipid peroxidation. The TBARS were measured following the modified protocol reported by Du and Bramlage, 1992 [40]. 150 mg of fresh plant leaves were ground in a chilled mortar with liquid nitrogen and extracted with 0.1% (*w*/*v*) trichloroacetic acid (TCA) solution. Following centrifugation (10,000× *g* at 4 °C for 10 min), an aliquot of 500 µL of supernatant was transferred to a fresh microcentrifuge tube and mixed with TBA solution [0.5% thiobarbituric acid in TCA 20% (*w*/*v*)] and then heated at 95 °C for 30 min. After incubation, the samples were chilled at 4 °C. The TBARS were measured at three wavelengths, 400, 532, and 600 nm, to discard any signal given by TBARS–sugar complexes.

2.5. Ascorbic Acid and Dehydroascorbic Acid Quantitation

The total ascorbate (Asc $_{tot}$) and dehydroascorbate (DHA) were measured as described by Gillespie and Ainsworth, 2007 [41]. 100 mg of shoot tissue was homogenized using a mortar and pestle cooled in liquid nitrogen and resuspended in 2.0 mL 6% (*w*/*v*) TCA solution, then transferred into a microcentrifuge tube. After centrifugation (13,000× *g* at 4 °C for 5 min), the supernatant was transferred to a new microcentrifuge tube. The reduced ascorbate (Asc $_{red}$) was determined in 100 µL of the supernatant mixed with 900 µL of developing reagent [TCA 2.5% (*w*/*v*), H_3PO_4 8.6% (*v*/*v*), α-α′ bipyridyl 0.08% (*w*/*v*) and $FeCl_3$ 0.3% (*w*/*v*)]. For Asc $_{tot}$ determination, 100 µL of supernatant was incubated with 50 µL of 10 mM DTT for 10 min and the reaction was stopped with 50 µL of 0.5% N-ethyl-maleimide. The absorbances of Asc $_{red}$ and Asc $_{tot}$ were measured at 525 nm in an UV/VIS spectrophotometer (Lambda EZ 210, Perkin Elmer, Waltham, MA, USA). These absorbances were used to calculate the ascorbate concentration using a calibration curve constructed with L-ascorbic acid (Asc $_{red}$, Sigma-Aldrich, St. Louis, MO, USA, A7506) treated with the developing reagent in the concentration range of 0.15 to 10 mM.

2.6. Quantitation of Oxidized (GSSG) and Reduced (GSH) Glutathione in Leaves of L. perenne

Approximately 200 mg of liquid nitrogen frozen leaves was ground with mortar and pestle and suspended with 800 µL of 5% *w*/*v* sulfosalicylic acid diluted in potassium phosphate EDTA buffer (KPE) [2.5 mM EDTA and 100 mM potassium phosphate pH 7.5], following centrifugation at 13,000× *g* at 4 °C for 20 min. Subsequently, 100 µL of supernatant was quickly mixed with 19.6 µL of 1.84 M triethanolamine. Amounts of total gluthatione (GSH $_{tot}$) and glutathione disulfide (GSSG) extracted from shoot tissues were carried out using a colorimetric microplate assay based in the protocol described Rahman et al [42], with glutathione reductase (GR, Sigma Aldrich), β-NADPH (MP Biomedicals, USA), and Ellman´s reagent [DNTB, 5,5′-dithiobis-(2-nitrobenzoic acid), Sigma-Aldrich]. Absorbance of the enzymatic assay 2-nitro-5-thiobenzoate (TNB) was measured at 412 nm. Calibration curves were made for GSH $_{red}$ and GSSG enzymatic assay substrates in ranges of (0 to 25 µM). Amounts of GSH $_{tot}$ and GSSG were used to compute the amount of reduced gluthathione (GSH $_{red}$).

2.7. Protein Extraction from L. perenne Leaf Tissue and Calculation of ROS Enzymatic Activities

For total protein extraction, 150 mg of plant leaves frozen in liquid nitrogen were ground via mechanical methods using a mortar and pestle. The lysate was then suspended in 2.0 mL of extraction buffer [50 mM potassium phosphate pH 7.0, 0.1% polyvinylpyrrolodine, and 0.01% Triton X-100] and centrifuged at 13,000× *g* at 4 °C for 10 min. The supernatant was used to measure the total protein concentration via the colorimetric method described by Bradford, 1976. The same samples were used to measure the SOD, APX, GR, and CAT enzyme activities. The SOD (E.C. 1.15.1.1) activity reaction was carried out with 60 µL of protein extract diluted to a 1.0 mL final volume with enzyme reaction buffer

[50 mM phosphate buffer pH 7.0, 13 mM methionine, EDTA 0.1 mM, and riboflavin 22 µM] and incubated with light irradiation (fluorescent tube of 40 W) for 10 min at 25 °C as described [43]. The blanks and controls were assayed without light irradiation. The total SOD enzyme activity was determined by monitoring the inhibition of nitroblue tetrazolium (NBT) reduction at 560 nm in a UV/VIS spectrophotometer (Lambda EZ 210, Perkin Elmer, Waltham, MA, USA). The SOD unit was established as the amount of SOD enzyme that is necessary to inhibit the NBT reduction to 50%. The enzymatic activity was normalized by total protein amount. An assessment of APX activity was carried out as described by Nakano Y and Asada K., 1981 [44]; the assay contained 125 µL of ascorbic acid [10 mM], 1 mL of phosphate buffer [50 mM, pH 7.0], 2.5 µL of 30% v/v H_2O_2, and 100 µL protein extract. The ascorbic acid oxidation was measured at 290 nm for 60 s in a spectrophotometer. The GR activity was based on the glutathione determination method described by Rahman et al., 2006 [42], using the Ellman´s reagent [5,5′-dithio-bis (2-nitrobenzoic acid)] that reacts with reduced glutathione (GSH). The enzyme activity was measured in 100 µL of protein extract suspended in KPE buffer, with 75 µL of DTNB [0.1 mM], 15 µL of GSSG [0.1 mM], and 30 µL of β-NADPH [0.1 M]; the reaction was measured at 412 nm for 120 s. To calculate catalase (CAT) enzymatic activity, the protocol described by Ambuko et al., 2013 [45] and Aebi, 1984 [46] was used. First, 100 µL of protein extract was used, then added to a reaction mix (100 µM H_2O_2 and 50mM phosphate buffer, pH 7). The reaction of H_2O_2 decomposition was spectrophotometrically measured for 60 s at a wavelength of 240 nm and calculated using a molar extinction coefficient of (39.4 mM^{-1} cm^{-1}). The amount of H_2O_2 degraded per second was determined and normalized to total protein in the extract.

2.8. Total RNA Extraction from Leaves of Lolium perenne and qRT-PCR Assays

The total RNA extraction was carried out following the Trizol®, (Invitrogen, Waltham, MA, USA) standard protocol. Then, 1 µg of total RNA was used for cDNA synthesis with a ThermoScript® Invitrogen Kit (Thermo, Waltham, MA, USA). The gene expression profiles were carried out via the SyBR Green qRT-PCR technique in an ABI7500 thermal cycler (Applied Biosystems, Foster City, CA, USA). The data were evaluated with LinReg software [47], and subsequently, the Ct values (threshold cycle) for each sample were used to estimate relative gene expression using the $2^{\Delta\Delta CT}$ algorithm described by Schmittgen and Livak, 2001 [48]. The gene expression was normalized using the 26 S proteosome subunit (26S) as the housekeeping gene. Detailed information of primers and PCR conditions are in Table 1 and the primers validation data are available in Supplementary File S2.

Table 1. List of primers used for qRT-PCR procedures.

Gene	Type	Sequence (5′->3′)	Tm (°C)	Product Size (pb)
26s proteosome subunit (26S)	Forward Reverse	TGCTTAGTTCCCCTAAGATAGTGA CTGAGACCAAACACGATTTCA	54	142
RuBisCO (RuBisCO)	Forward Reverse	TCATATCGAGCCTGTTGCTG AGAGCACGTAGGGCTTTGAA	60	144
Chlorophyll A binding protein (ChlAbp)	Forward Reverse	GCGCTCGGCCTATAATCTAC AACACACCACCCGAAAGAAG	60	170
Ferredoxin (Fered)	Forward Reverse	CGTCATCGAGACCCACAAGG GGTGGCGATGCCCATGTA	58	93
Copper–zinc superoxide dismutase (Cu/Zn-SOD)	Forward Reverse	CTCTTGCTAAGCTCATGTCC TCCTGGACTTCATGGCTTC	57	49
Iron superoxide dismu-tase (Fe-SOD)	Forward Reverse	GAAGCATCAGCAGGATCAC GTTAACTACCGAGAGTTTCCTC	58	70
Ascorbate peroxidase (APX)	Forward Reverse	GCTCTATCTGGTGGCCACAG TCAGAGGATCACGGGTCCAT	57	82
Glutathione reductase (GR)	Forward Reverse	TATCCGTCGTGGGTCTCAGT GACAGACTTCTCCTGCCGTT	57	84

2.9. Statistical Analysis

This study was carried out through seven experimental replicates and three analytical replicates for each evaluated parameter. The values are expressed as mean ± standard error (ES) using Microsoft Excel 365 (Microsoft Corporation, Seattle, WA, USA). The effects of sulfate supply in the presence of Al^{3+} toxicity on the evaluated parameters were analyzed via one- or two-way ANOVA using Sigma Plot 13.0 software (Systat software, San Jose, CA, USA) (Supplementary Tables S1 and S2) [18]. For multiple comparison, the means were compared using Sidak's or Tukey test as appropriate ($p \leq 0.05$).

3. Results

3.1. Sulfate Supplementation Modulates Total Proteins, Calcium, Magnesium and TBARs Concentration in Leaves of Plants Subjected to Al^{3+} Toxicity

A total protein quantitation was performed to evaluate the physiological effects of sulfate amendments after 48 h of exposure to Al^{3+} -toxicity. These results show a significant decrease in total protein amount in plant leaves grown in 120 µM sulfate in presence of Al^{3+}-toxity ($p < 0.01$) compared to control with no Al^{3+}-toxicity. A similar result, but in smaller magnitude, was observed in the leaves of plants grown with 240 µM sulfate in Al^{3+} ($p < 0.05$). No changes in protein amount were observed in the leaves of plants exposed to Al^{3+} toxicity grown in 360 µM sulfate (Figure 1A).

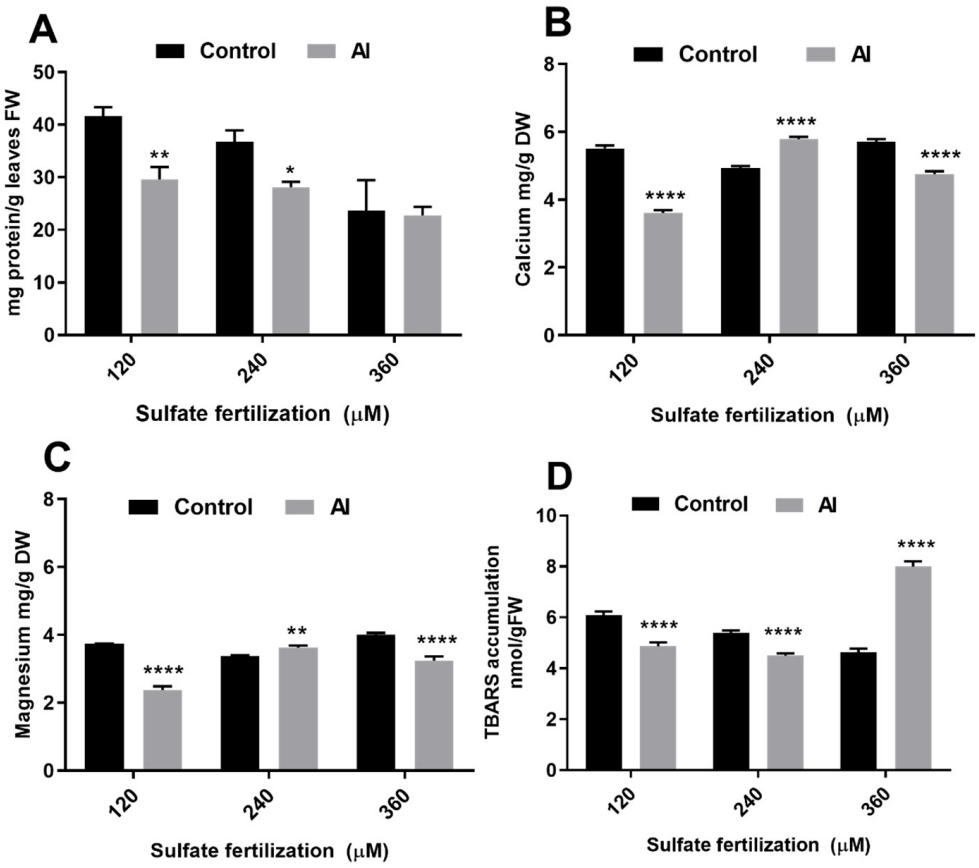

Figure 1. Total protein, Ca, Mg, and TBARS concentrations in leaves of perennial ryegrass shoots cultured at increased sulfate supply after 48 h with or without Al^{3+}-toxicity. Total protein (**A**), calcium (**B**), magnesium (**C**) and TBARS (**D**) in control (black bars) or Al^{3+}-treated (gray bars) *L. perenne* grown in the respective sulfate amendments (120, 240, 360 µM). Two-way ANOVA and Sidak's test (*p* values: * <0.05; ** <0.01; and **** <0.001) provided evidence of significant differences.

Calcium and magnesium amounts were quantified in plant leaves grown in different sulfate nutrition conditions in the presence of Al^{3+}-toxicity for 48 h. The results show a significant decrease in calcium and magnesium amounts in plant leaves grown with 120 or 360 µM sulfate fertilization when Al^{3+}-toxicity was present ($p < 0.001$). Contrarily, a significant increase in calcium ($p < 0.001$) and magnesium ($p < 0.05$) amounts were observed in plants grown with 240 µM sulfate and Al^{3+} (Figure 1B,C).

A TBARS assay was performed to analyze the ability of sulfate amendments to reduce the adverse effects of Al^{3+} toxicity at 28 h of exposure on leaves of *L. perenne cv. Jumbo*. The results show a decrease in TBARS production in plant leaves grown with 120 or 240 µM sulfate and Al^{3+}-toxicity ($p < 0.001$). Contrarily, a significant increase in TBARS level was observed in the leaves of plants grown with 360 µM sulfate in the presence of Al^{3+} ($p < 0.001$) (Figure 1D).

3.2. Sulfate Supplementation Modulated Photosynthetic Response in Leaves of Plants Subjected to Al^{3+} Toxicity

The analysis of both photosynthetic pigments, total amounts chlorophyll and carotenoids, showed similar patterns. A decrease in total chlorophyll was observed in the leaves of plants grown with 120 ($p < 0.01$) or 240 µM ($p < 0.001$) sulfate exposed to Al^{3+}-toxicity for 48 h; however, the opposite effect was observed in plants grown with 360 µM sulfate ($p < 0.001$) (Figure 2A). The analysis of carotenoids showed a decrease in the leaves of plants grown with 120 ($p < 0.05$) or 240 µM ($p < 0.001$) sulfate when Al^{3+}-toxicity was present for 48 h; however, the opposite effect was observed in plants grown with 360 µM sulfate ($p < 0.001$) (Figure 2B). Interestingly, the chlorophyll A/B ratio, an indicator of cellular stress, showed no changes in plants grown with 120 or 240 µM sulfate exposed to Al^{3+}-toxicity for 48 h, but an important decrease in the chlorophyll A/B ratio in the plant leaves of *L. perenne* grown with 360 µM sulfate in the presence of Al^{3+}-toxicity for 48 h compared with their respective controls suggests modifications in the photosynthetic system responses (Figure 2C).

To evaluate the outcome of sulfate nutrition on Al^{3+}-toxicity at the transcriptional level, we measured gene expression for proteins involved in different phases of photosynthesis such as ribulose-1,5-bisphosphate carboxylase/oxygenase (RuBisCO), chlorophyll A binding protein (ChlAbp), and ferredoxin (Fered). The data collected in Table 2 represent gene expression profiles expressed as Al^{3+}/control ratio for every sulfate concentration. In the presence of Al^{3+}-toxicity, important increases in the expression of every analyzed gene, RuBisCO, ChlAbp, and Fered, were observed in plant leaves grown with 120 µM sulfate ($p < 0.05$). Interestingly, no changes in gene expression levels were detected for any of the analyzed genes in plant leaves grown with 240 µM sulfate. No changes were observed in the expression of RuBisCO and ChlAbp genes in plants grown with 360 µM sulfate; however, Fered gene expression significantly decreased in that same condition ($p < 0.05$).

Table 2. Gene expression analysis for proteins involved in photosynthesis mechanism response in leaves of Al^{3+}-toxicity treated *L. perenne cv. Jumbo*. Al/control expression ratio of RuBisCO, ChlAbp (chlorophyll A binding protein), and Fered (ferredoxin) for every sulfate condition are shown. One-way ANOVA was carried out and significant differences with Tukey's post-test between sulfate conditions are highlighted with asterisks (* $p < 0.05$).

Sulfate Nutrition (µM)	RuBisCO	ChlAbp	Fered
120	7.54 * ± 2.20	11.49 * ± 3.96	2.24 * ± 0.40
240	1.84 ± 1.09	1.17 ± 0.55	1.12 ± 0.15
360	1.54 ± 0.24	1.30 ± 0.20	0.26 * ± 0.02

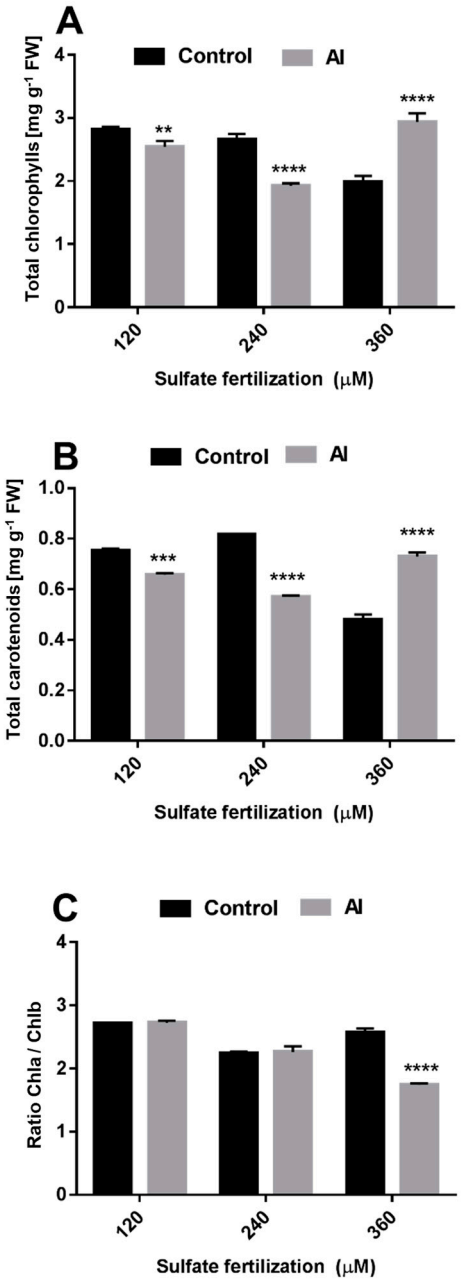

Figure 2. Sulfate nutrition modulates photosynthetic pigment amounts in shoots of *L. perenne cv. Jumbo* after 48 h of Al^{3+}-toxicity exposure. Total chlorophyll (**A**), carotenoids (**B**), and chlorophyll A/B ratio (**C**) in leaves of *L. perenne* grown with different sulfate amendments (120, 240 or 360 μM) in absence (black bars) or presence (grey bars) of Al^{3+} toxicity. The values reported are means ± SE (n = 3). Two-way ANOVA and Sidak's test were carried out (*p* values: ** <0.01; *** <0.005; and **** <0.001). Asterisks show statistical differences between Al and control for every sulfate condition.

3.3. Sulfate Supply Modulates Antioxidant Metabolites in Shoots of L. perenne cv. Jumbo Exposed to Al^{3+} Toxicity

Due to their close relationship in the Halliwell–Asada cycle, ascorbate and glutathione species were quantified as described by Gillespie and Ainsworth et al., 2007 and Rahman et al., 2006 [41,42], respectively. In general, the results show variations in both glutathione and ascorbate species; however, the effects of sulfate supplementation were significantly more drastic for glutathione species, compared to ascorbate species. In detail, total ascorbate (Asc_{tot}) decreased in plant leaves grown in the presence of Al^{3+}-toxicity with 120 or 240 μM sulfate ($p < 0.001$); however, the opposite effect was observed in the leaves of plants grown

with 360 μM sulfate ($p < 0.01$) (Figure 3A). Reduced ascorbate ratio (Asc $_{red}$ /Asc $_{tot}$), an indicator of plant cell redox homeostasis status, displayed a similar pattern to those previously described, showing a decrease in plant leaves grown in the presence of Al^{3+}-toxicity along with 120 ($p < 0.01$) and 240 μM sulfate supply ($p < 0.05$), but not at 360 μM sulfate treatment (Figure 3C). On the other hand, total glutathione species (GSH $_{red}$ + GSSG, or [GSH $_{tot}$]) decreased in plant leaves grown in 120 or 360 μM sulfate in the presence of Al^{3+}-toxicity ($p < 0.005$); contrarily, GSH $_{tot}$ increased two times in the leaves of plants grown with 240 μM sulfate ($p < 0.001$) as compared to their respective controls in the absence of aluminum (Figure 3B). Interestingly, GSH $_{red}$ ratio, expressed as (GSH $_{red}$/ GSH $_{tot}$), were at least 1.4 folds more in plant leaves grown with 120 or 360 μM sulfate and Al^{3+}-toxicity ($p < 0.001$ and 0.05, respectively), compared to the respectively tissue of control plants without Al^{3+}-toxicity, but the opposite effect was observed in plant leaves grown with 240 μM sulfate exposed to Al^{3+}-toxicity ($p < 0.001$) (Figure 3D).

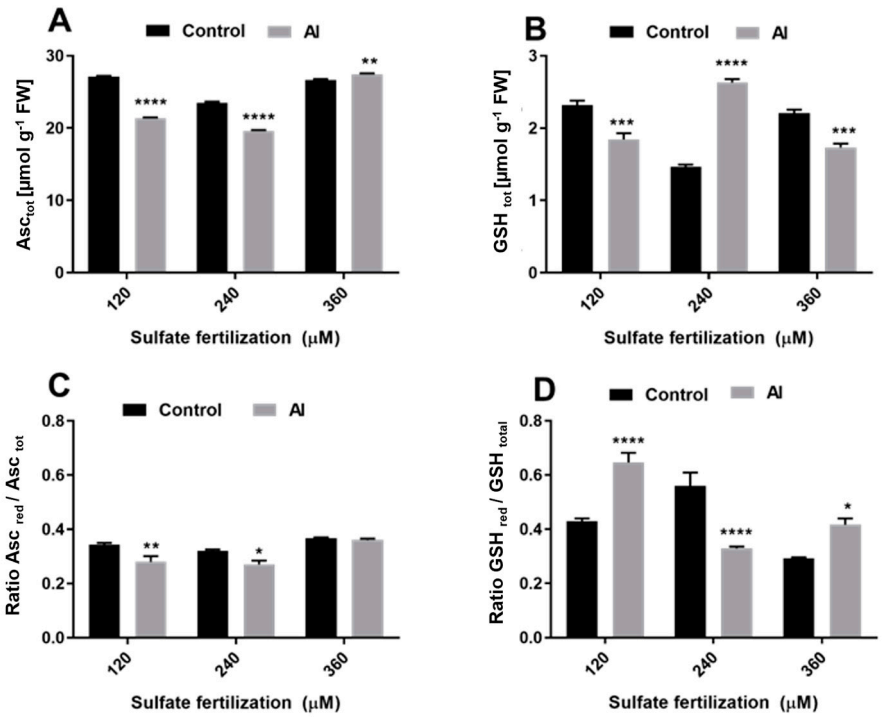

Figure 3. Sulfate-nutrition-modulated redox status of antioxidant metabolites, ascorbate, and glutathione species in shoots of *L. perenne cv. Jumbo* after 48 h of Al^{3+}-toxicity exposure. Total ascorbate [Asc $_{tot}$] (**A**), total glutathione [GSH $_{tot}$] amounts (**B**), reduced ascorbate ratio (**C**) and reduced glutathione ratio (**D**) in leaves of *L. perenne* grown in different sulfate amendments (120, 240 or 360 μM) and in absence (black bars) or presence (grey bars) of 48 h Al^{3+}-toxicity. TWO-WAY-ANOVA and Sidak's test were carried out (p values: * <0.05; ** <0.01; *** <0.005 and **** <0.001). Asterisks show statistical differences for every sulfate condition. The value reported are mean ± SE (n = 3).

3.4. Sulfate Supplementation Modulates Enzyme Activity and Gene Expression of ROS Scavenging Enzymes in Shoots of L. perenne cv. Jumbo Exposed to Al^{3+} Toxicity

Ascorbate peroxidase (APX), glutathione reductase (GR), and superoxide dismutase (SOD), and Catalase (CAT), total enzymatic activities, and gene expression profiles of representative isoenzymes ROS scavenging proteins, were analyzed to evaluate their involvement in cell defense against reactive oxygen species (ROS) derived of short-term Al^{3+}-toxity of plant leaves. SOD activity showed notable differences depending on sulfate supply amounts, showing a dramatic decrease in leaves grown with 120 μM sulfate with Al^{3+}-toxicity ($p < 0.005$); by the contrary, we observed increased SOD activity in leaves of plants grown with 360 μM sulfate exposed Al^{3+} -toxicity ($p < 0.05$) as compared to their respective controls. No statistical difference in SOD activity was observed in plants grown

with 240 µM sulfate (Figure 4A). In addition, a similar profile was observed in APX enzyme activity, showing a decrease in APX activity in the leaves of plants grown with 120 µM sulfate when Al^{3+}-toxicity was present ($p < 0.005$); on the contrary, a two-fold increase was detected in the leaves of the plants grown with 360 µM sulfate and Al^{3+}-toxicity ($p < 0.001$), and again, no changes were observed in plants grown with 240 µM sulfate and exposed to Al^{3+}-toxicity (Figure 4B). Finally, GR enzyme activity showed a decrease in the leaves of plants grown with 120 or 360 µM sulfate and Al^{3+}-toxicity ($p < 0.01$); the opposite effect, a two-fold increase ($p < 0.01$), was observed in the leaves of plants grown with 240 µM sulfate compared to their respective controls (Figure 4C). On the contrary, an increase in catalase activity was detected in the plants exposed to 120 and 360 µM sulfate in the presence of Al^{3+} toxicity ($p < 0.001$ and 0.05, respectively); nevertheless, 240 µM of sulfate showed less activity (Figure 4D), and a similar pattern was observed in SOD activity.

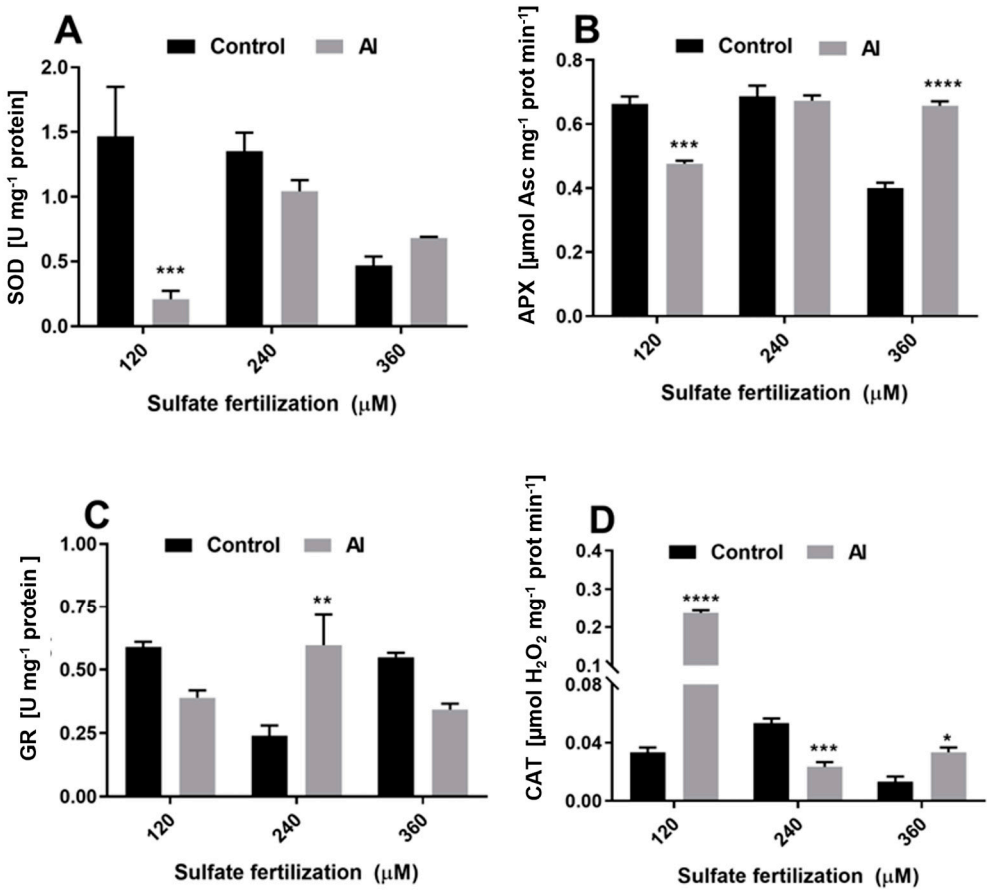

Figure 4. Sulfate nutrition recovers enzymatic activities involved in ROS detoxification mechanism when *L. perenne cv. Jumbo* is exposed to 48 h Al^{3+}-toxicity. Superoxide dismutase, SOD (**A**), ascorbate peroxidase, APX (**B**), glutathione reductase, GR (**C**), and catalase (CAT) (**D**). Leaves of perennial ryegrass in absence (black bars) or presence of Al^{3+}-toxicity (grey bars) grown in three different sulfate conditions (120, 240, or 360 µM) were considered. Two-way ANOVA and Sidak's test were carried out (p values: * <0.05; ** <0.01; *** <0.005; and **** <0.001). Asterisk shows statistical differences between Al and control for every sulfate condition. The values reported are means ± SE (n = 3).

The gene expression profiles of enzymes involved in ROS detoxification are shown in Table 3. Interestingly, Fe-SOD and APX gene expression level increased in the leaves of plants grown with 120 µM sulfate concentration and exposed to Al^{3+}-toxicity ($p < 0.05$). In addition, a significant decrease in Fe-SOD and APX gene expression level were observed in the leaves of plants grown with 360 µM sulfate in the presence of Al^{3+}-toxicity ($p < 0.05$). No changes were observed for Cu/Zn-SOD or GR for every sulfate condition. Also, no changes were observed for any of the evaluated genes in plants grown with 240 µM sulfate.

Table 3. Gene expression profiles of enzymes involved in ROS detoxification mechanism in leaves. Al^{3+}/control ratios of Fe-SOD (iron superoxide dismutase), Cu/Zn SOD (copper/zinc superoxide dismutase), APX (ascorbate peroxidase), and GR (glutathione reductase) are shown in every sulfate condition. One-way ANOVA was carried out and significant differences with Tukey post-test between sulfate conditions are highlighted with asterisks (* $p < 0.05$).

Sulfate Nutrition (μM)	Fe-SOD	Cu/Zn SOD	APX	GR
120	1.69 * ± 0.26	0.86 ± 0.15	1.63 * ± 0.34	0.93 ± 0.16
240	1.27 ± 0.13	1.11 ± 0.11	0.98 ± 0.03	1.01 ± 0.03
360	0.47 * ± 0.12	0.60 ± 0.12	0.47 * ± 0.07	0.80 ± 0.07

4. Discussion

It has been described that some of the adverse effects produced by Al^{3+}-toxicity in root tissue can be ameliorated by the administration of sulfate amendments, improving soil nutrient uptake and plant growth [8,9,49]. Nevertheless, few data reported the effects of sulfate amendments being able to ameliorate symptoms induced by trivalent aluminum (Al^{+3}) in leaves [18,32,36], despite aluminum inducing negative effects in leaves after short-term and long-term exposures [11,19,50,51]. The current study demonstrates that the proper amount of sulfate nutrition ameliorates the effects of aluminum stress in plant leaves, improving mineral uptake, photosynthetic response, and the enhancement of ROS scavenging mechanisms

4.1. Adequate Sulfate Supply Recovered Membrane Damage, and Mineral Uptake; but Not Total Protein Amount after Al^{3+} Toxicity Exposure

To verify the effects of short-term Al^{3+}-toxicity in leaves along with evaluating the role of sulfate to ameliorate Al^{3+}-toxicity symptoms, we evaluated different physiological parameters such as total protein concentration, membrane damage, and Ca and Mg uptake, previously reported as possible targets of Al^{3+}-toxicity [12,18,24].

On one first assessment of the experiment, no morphological changes were observed after 48 h in leaves of *L. perenne* plants cultivated in combined conditions of increasing sulfate supply and short-term Al^{3+}-toxicity, that was additionally corroborated by dry mass percentage, fresh weight, and dry weight measurements (Supplementary Figure S1). After 48 h of Al^{3+}-toxicity exposure, significant amounts of total aluminum were found in leaves of plants grown in all the experimental treatments of sulfate combined with Al^{3+}-toxicity, compared to their respective sulfate supply without Al^{3+}-treatment (Supplementary Figure S2A); but, these Al amounts were ten times smaller than those accumulated in root tissue after 48 h in the same experimental conditions reported previously by our group [32]. However, regardless of the small concentration of Al detected in the plant leaves after 48 h of treatment, a significant antioxidant response was observed. To evaluate the effect of sulfate addition on some physiologic parameters affected by Al^{3+}-toxicity, total sulfur contents were measured in every experimental condition. After 48 h, a progressive increase in the concentrations of total sulfur was determined in the leaves of plants treated with increased sulfate supply concentrations. Remarkably, Al^{3+}-toxicity treatment causes a significant sulfur accumulation in leaves compared to controls, and this increase is modulated in a dose dependent manner (Supplementary Figure S2B). Similar patterns in SO_4^{2-} content were observed in *A. thaliana*, and *N. tabacum* cultured in combined conditions of increasing sulfate supply and long-term cadmium toxicity [52]. In detail, an increase in sulfate nutrition from 120 to 360 μM was not effective to restore total protein amount in plant leaves of Al^{3+}-treated plants; this is a key point due to high-protein content in crops are relevant for human and livestock nourishment. Our results are similar to previously reported data where sulfur supplementation improved crop yield and protein concentration in wheat [53], *Citrus grandis* leaves [24], and Perennial ryegrass [18], as an increase in sulfur concentration improved soluble protein amount; but not when Al^{+3}-toxicity

is presented. Nevertheless, short term-Al^{3+} toxicity inhibited the protein yield in *L. perenne* leaves of plants cultivated on the three sulfate supply treatments used in the experiment.

In view of the important functions of Ca^{2+} in plant metabolism, such as cell wall and membrane formation and molecular messenger production, several studies suggested that Al^{3+} toxicity generates a reduction in mineral uptake and translocation from roots to other plant organs [54], having a stronger effect on Ca^{2+} and Mg^{2+} uptake than other minerals, showing reductions of 61% and 72%, respectively, in 10 different maize genotypes [55]. In addition, short-term growth studies demonstrated that the additions of Ca^{2+}, Mg^{2+}, and Sr^{2+} were equally effective in alleviating Al^{3+} toxicity symptoms [30,54]. On the other hand, sulfur administration was able to improve nutrient uptake in olive fruits and wheat [56,57]. Additionally, recent studies demonstrated that sulfate amendments, such as gypsum, improve plant growth through soil structure stabilization, enhancing cation exchange capacity and increasing magnesium and calcium availability [58,59]; moreover, SO_4^{2-} fertilizers prevent cadmium and arsenic availability in paddy fields used to grow rice, giving insight on the use of sulfate to improve crop production [60,61]. In the present study, we observed a reduction in Ca^{2+} and Mg^{2+} amounts in the leaves of *L. perenne cv Jumbo* grown with 120 and 360 µM sulfate and exposed to Al^{3+} after 48 h. On the contrary, increased Ca^{2+} and Mg^{2+} amounts were observed in the leaves of plants grown with 240 µM sulfate and exposed to Al^{3+} toxicity. In addition, these increases in Ca^{2+} and Mg^{2+} amounts were accompanied by a decrease in TBARS accumulation in plants grown in the same experimental conditions. Similar results were observed by Wulff et al., 2014 [18], showing the lowest TBARS levels in *L. perenne cv. Jumbo* grown in 240 µM sulfate after 28 days of exposure to Al^{3+}. The benefits of sulfur supplementation were also observed by Guo et al., 2017 [24], in which an increase in S supply of 1 mM may cause a decrease in TBARS accumulation in *Citrus grandis* exposed to aluminum toxicity.

In this respect, it has been previously reported that Al^{3+} accumulates in the cell wall, mostly interacting with pectin [62–64] and displacing Ca^{2+}, an essential macronutrient element for plant cell wall stability [8]. In addition, Al^{3+} may also cause the displacement of Ca^{2+} from interacting with phospholipids in biological membranes, showing an important reduction in membrane fluidity [65,66]. On the other hand, Mg^{2+} plays a central function in several metabolic processes such as being a cofactor of enzyme activity with ATP and being the central atom in chlorophylls; therefore, Mg^{2+} deficiency is the most important candidate to cause a reduction in chlorophyll synthesis (chlorosis), ROS production, and metal accumulation [67]. All these data together suggest that an adequate amount of sulfate is necessary to maintain Ca^{2+} and Mg^{2+} concentrations along with their cell metabolic functions close to normal and therefore ameliorate Al^{3+} toxicity symptoms. However, as previously reported, an excessive increase in sulfur can cause severe adverse effects [18,68].

4.2. Adequate Sulfate Supplementation Was Able to Maintain Photosynthetic Parameters in Leaves of L. perennial cv. Jumbo Exposed to Al^{3+} Toxicity

A significant decrease in total chlorophyll and carotenoids after 48 h of exposure to different Al^{3+} concentrations was observed in three blueberry varieties most frequently cultivated in southern Chile [19,20]; additionally, reduction in photosynthetic pigments were observed in Eucaliptus clones, caused by 1-day exposure to 4.4 mM Al^{3+} toxicity [51]. In addition, studies in citrus species show that Al^{3+} toxicity causes decreases in stomatal conductance and total protein in foliar tissues at a maximum 1.4 mM aluminum concentration for 18 weeks [69]. However, those studies did not consider the effect of plant sulfate nutrient status as a modulator against Al^{3+} toxicity.

The present study demonstrates a decrease in both total chlorophyll and carotenoids in plants grown with 120 or 240 µM sulfate and exposed to Al^{3+}-toxicity by 48 h. Interestingly, chlorophyll A/B ratio, a plant photosynthetic stress indicator, showed no change for these same experimental conditions. On the other hand, the opposite effect was observed in plants grown with 360 µM sulfate and exposed to Al^{3+}-toxicity, showing an important increase in total chlorophyll and carotenoids, along with a significant decrease in chlorophyll

A/B ratio. In this respect, a decrease in chlorophyll A/B ratio has been associated with oxidative stress in plants subjected to abiotic stresses such as light or nitrogen deficiency and paraquat [70,71]. The observed chlorophyll A/B ratio suggests that a 360 µM sulfate supply could be in excess, having no effect to ameliorate Al^{3+}-toxicity symptoms. These results are supported by the gene expression of proteins involved in photosynthesis such as RuBisCO, ChlAbp, and Ferred. Plants grown with 120 µM sulfate with Al^{3+}-toxicity showed an increase in gene expression; however, plants cultured with higher amounts of sulfate showed values close to 1 for RuBisCO and ChlAbp, suggesting that sulfate in a proper amount can prevent changes in photosynthetic response induced by aluminum stress. These data are supported by Guo et al., 2017 [24] showing that 1.0 mM sulfur amendment plays an important role in the alleviation of 1 mM $AlCl_3$ exposure by improving pigment concentration and photosynthetic efficiency in Citrus grandis after 18 weeks. On the other hand, Filipovic and Jovanović, 2017 [68] demonstrated that an excess of hydrogen sulfide plays a phytotoxic effect in several plant species. In addition, an optimal N/S ratio near to 14/1 is required for wheat and perennial ryegrass growth [72]. In summary, a high N/S ratio due to S deficiency may cause lower N availability and therefore a subsequent disruption in amino acids/protein metabolism in plants [73], giving important clues about the role of sulfur balance in preventing or alleviating the effects of Al^{3+} toxicity response at a physiological level. In this study, an important response in plant leaves grown with 240 µM sulfate exposed to Al^{3+}-toxicity was observed in *L. perenne cv. Jumbo.* In this condition, 16.47 µmoles/plant of sulfur availability and 275.19 µmoles/plant of nitrogen were observed [32]; thus, 240 µM sulfate provides a N/S ratio of 16/1, very similar to that described as an adequate N/S for ryegrass. These data together support the hypothesis that a proper nutrient ratio is important for plant growth; thus, a suitable sulfur amendment among plant species may vary, and in this context 240 µM provides a good response for *L. perenne cv. Jumbo***.** Instead, 1 mM sulfur fertilization is suitable for *Citrus grandis* growth, and additionally, 45 kg S ha^{-1} is recommended to obtain a maximum yield in tobacco crops. Therefore, a specific analysis of the proper amount of sulfur supply to improve culture production must be carried out [74].

4.3. Sulfate Supplementation Activates ROS Defense Mechanism in Leaves of L. perennial cv. Jumbo Exposed to Al^{3+} Toxicity

In plant cells, oxidative stress occurs mainly due to electron decoupling from biochemical redox processes of photosynthesis as well as mitochondrial cellular respiration [75,76]. Imbalance in electron-transport chains as well as ROS production are secondary symptoms of Al^{3+}-toxicity able to activate antioxidant mechanisms. The antioxidant machinery is mainly composed of biomolecules such as ascorbic acid and glutathione, which help to maintain intracellular redox balance, which can transform ROS species into less toxic species. In detail, glutathione can act as a secondary substrate that allows for the recycling of ascorbic acid used for H_2O_2 catabolism by ascorbate peroxidase, which comprises the Halliwell–Asada–Foyer cycle metabolic pathway. Furthermore, this ROS scavenging enzymatic cycle is very close to photosystems to overcome probable electron leaks from electron transport chain due to abiotic stress [77–79]. In this respect, long-term Al^{3+}-stress (14-21 days) causes increasing lipid peroxidation, and ROS production in tomato and wheat leaves, respectively [6,17,80]. On the other hand, Vera-Villalobos et al., 2020 and D. B. Zhu et al., 2015 [32,81] demonstrated the effects of sulfate in roots, reducing the ROS damage caused by a short-term Al^{3+}-toxicity response (48 h) in wheat grains and *L. perenne cv. Jumbo*. The present data demonstrated that 240 µM sulfate fertilization was the optimal amount to modulate the antioxidant response in the leaves of plants exposed to 48 h of Al^{3+} -toxicity, and the effect of this macronutrient was mainly focused on the regulation of SOD and APX enzyme activities and their gene expression, along with the redox status of antioxidant metabolites, modulating glutathione rather than ascorbate. These results are related to those observed by Wulff-Zottele et al., 2014 [18], in which a sulfate-dependent response was observed after 28 days of exposure to Al^{3+}-toxicity, playing an important role in TBARS

and ROS scavenging enzymes regulation and the glutathione redox balance. Similarly, hydrogen sulfide (H_2S; a cell signaling molecule) modified ROS scavenging enzymatic activity, like catalases, peroxidases, and SOD dismutases [35]. However, Filipovic and Jovanovic., 2017 [69] described that an excess of H_2S inhibits plant growth.

5. Conclusions

In summary, the present study is the first to demonstrate that sulfate metabolism has a fundamental function in modulating the response against stress caused by short-term Al^{3+}-toxicity in the aerial tissue of *L. perenne cv. Jumbo* (Figure 5). Even when long-term Al^{3+}-toxicity is a well-characterized event that produces drastic effects on plants, the antioxidant response is a rapid event that might be appreciated at 48 h of this metal toxicity exposure; additionally, sulfate plays an important role to maintain the redox equilibrium and counteract early symptoms of Al^{3+}-toxicity. However, every plant species possesses different culture condition and soil preferences; thus, a specific analysis of the proper amount of sulfate supplementation to ameliorate Al^{3+} symptoms must be established for each plant species, because, according to our previous data, an excess of sulfate may cause adverse physiological effects.

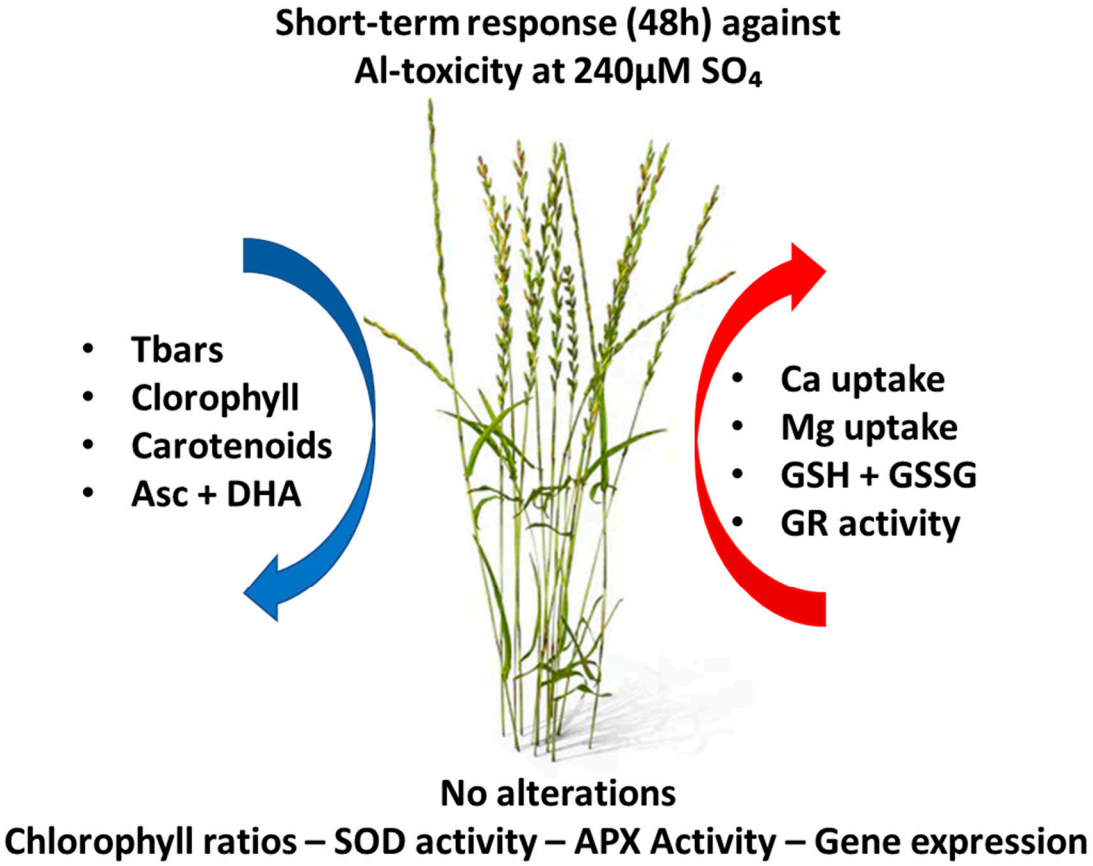

Figure 5. Representation of sulfate effects against short-term Al^{3+}-toxicity in leaves of *L. perenne cv. Jumbo*. These changes were observed in 240 µM of SO_4^{2-} as an adequate sulfate condition.

Supplementary Materials: The following supporting information can be downloaded at: https://www.mdpi.com/article/10.3390/agriculture14091506/s1, Table S1: Two-way ANOVA values. letters denote statistical differences caused by the analyzed factor; Table S2: Two-way ANOVA values. Letters denote statistical differences caused by factors; Figure S1: Fresh dry leaf weights exposed to short-term Al^{3+}-toxicity; Figure S2: Aluminum and sulfate content in plant leaves.

Author Contributions: Conceptualization: C.W.-Z. and A.M.-S.; methodology, C.W.-Z., A.M.-S., D.R.-S., L.L.-D. and H.V.-V.; software, C.W.-Z. and H.V.-V.; validation, C.W.-Z., A.M.-S. and H.V.-V.;

formal analysis, C.W.-Z., A.M.-S., A.S.G., L.L.-D. and H.V.-V.; investigation, C.W.-Z., A.M.-S., A.S.G., D.R.-S., L.L.-D. and H.V.-V.; resources, C.W.-Z. and A.M.-S.; data curation, C.W.-Z.; writing—original draft preparation, H.V.-V., C.W.-Z. and A.S.G.; writing—review and editing, C.W.-Z., A.M.-S., and H.V.-V.; visualization, H.V.-V., L.L.-D. and C.W.-Z.; supervision, C.W.-Z., A.M.-S. and D.R.-S.; project administration, C.W.-Z. and A.M.-S.; funding acquisition, C.W.-Z. and A.M.-S. The MSc of Biotechnology thesis of L.L.-D. at the Universidad de Antofagasta is partially based on this work. The Ph.D. of Cell Biology thesis of H.V.-V. at the Universidad de Antofagasta is also partially based on this work. All authors have read and agreed to the published version of the manuscript.

Funding: This work was supported by Grant N° 1130655 FONDECYT Chile, directed by Dr. Cristián Wulff-Zottele (Principal Investigator) and Dr. Ana Mercado Seguel (Second Investigator). Proyecto semillero VRIIP-DGI-UA °5310, directed by Dr. Ana Mercado (Principal Investigator) and Dr. Cristián Wulff-Zottele (Associate Investigator).

Data Availability Statement: Enquiries about data availability should be directed to Cristián Enrique Wulff-Zottele (cristian.wulff.z@uantof.cl).

Acknowledgments: This manuscript is dedicated to the deceased Domingo Román-Silva, emeritus professor of the Chemistry Department of Universidad de Antofagasta. We acknowledge his analytical chemistry expertise, and in life comments of the work developed and showed in this paper.

Conflicts of Interest: The authors declare no conflicts of interest.

References

1. von Uexküll, H.R.; Mutert, E. Global Extent, Development and Economic Impact of Acid Soils. *Plant Soil* **1995**, *171*, 1–15. [CrossRef]
2. Raza, S.; Zamanian, K.; Ullah, S.; Kuzyakov, Y.; Virto, I.; Zhou, J. Inorganic Carbon Losses by Soil Acidification Jeopardize Global Efforts on Carbon Sequestration and Climate Change Mitigation. *J. Clean. Prod.* **2021**, *315*, 128036. [CrossRef]
3. Nachtergaele, F. Soil Taxonomy—A Basic System of Soil Classification for Making and Interpreting Soil Surveys. *Geoderma* **2001**, *99*, 336–337. [CrossRef]
4. Aguilera, S.M.; Borie, G.; Peirano, P.; Galindo, G. Organic Matter in Volcanic Soils in Chile: Chemical and Biochemical Characterization. *Commun. Soil Sci. Plant Anal.* **1997**, *28*, 899–912. [CrossRef]
5. Shetty, R.; Vidya, C.S.N.; Prakash, N.B.; Lux, A.; Vaculík, M. Aluminum Toxicity in Plants and Its Possible Mitigation in Acid Soils by Biochar: A Review. *Sci. Total Environ.* **2021**, *765*, 142744. [CrossRef] [PubMed]
6. Yamamoto, Y. Aluminum Toxicity in Plant Cells: Mechanisms of Cell Death and Inhibition of Cell Elongation. *Soil Sci. Plant Nutr.* **2019**, *65*, 41–55. [CrossRef]
7. Poschenrieder, C.; Gunsé, B.; Corrales, I.; Barceló, J. A Glance into Aluminum Toxicity and Resistance in Plants. *Sci. Total Environ.* **2008**, *400*, 356–368. [CrossRef]
8. Matsumoto, H. Cell Biology of Aluminum Toxicity Tolerance in Higher Plants. *Int. Rev. Cytol.* **2000**, *200*, 1–46.
9. Llugany, M.; Poschenrieder, C.; Barceló, J. Monitoring of Aluminium-induced Inhibition of Root Elongation in Four Maize Cultivars Differing in Tolerance to Aluminium and Proton Toxicity. *Physiol. Plant.* **1995**, *93*, 265–271. [CrossRef]
10. Silva, I.R.; Smyth, T.J.; Moxley, D.F.; Carter, T.E.; Allen, N.S.; Rufty, T.W. Aluminum Accumulation at Nuclei of Cells in the Root Tip. Fluorescence Detection Using Lumogallion and Confocal Laser Scanning Microscopy. *Plant Physiol.* **2000**, *123*, 543–552. [CrossRef]
11. He, H.; Li, Y.; He, L.F. Aluminum Toxicity and Tolerance in Solanaceae Plants. *S. Afr. J. Bot.* **2019**, *123*, 23–29. [CrossRef]
12. Cartes, P.; McManus, M.; Wulff-Zottele, C.; Leung, S.; Gutiérrez-Moraga, A.; Mora, M. de la L. Differential Superoxide Dismutase Expression in Ryegrass Cultivars in Response to Short Term Aluminium Stress. *Plant Soil* **2012**, *350*, 353–363. [CrossRef]
13. Frantzios, G.; Galatis, B.; Apostolakos, P. Aluminium Effects on Microtubule Organization in Dividing Root-Tip Cells of Triticum Turgidum. II. Cytokinetic Cells. *J. Plant Res.* **2001**, *114*, 157–170. [CrossRef]
14. Horst, W.J.; Wang, Y.; Eticha, D. The Role of the Root Apoplast in Aluminium-Induced Inhibition of Root Elongation and in Aluminium Resistance of Plants: A Review. *Ann. Bot.* **2010**, *106*, 185–197. [CrossRef] [PubMed]
15. Yin, L.; Mano, J.; Wang, S.; Tsuji, W.; Tanaka, K. The Involvement of Lipid Peroxide-Derived Aldehydes in Aluminum Toxicity of Tobacco Roots. *Plant Physiol.* **2010**, *152*, 1406–1417. [CrossRef]
16. Yamamoto, Y.; Kobayashi, Y.; Matsumoto, H. Lipid Peroxidation Is an Early Symptom Triggered by Aluminum, but Not the Primary Cause of Elongation Inhibition in Pea Roots. *Plant Physiol.* **2001**, *125*, 199–208. [CrossRef] [PubMed]
17. Yamamoto, Y.; Kobayashi, Y.; Devi, S.R.; Rikiishi, S.; Matsumoto, H. Aluminum Toxicity Is Associated with Mitochondrial Dysfunction and the Production of Reactive Oxygen Species in Plant Cells. *Plant Physiol.* **2002**, *128*, 63–72. [CrossRef]
18. Wulff-Zottele, C.; Hesse, H.; Fisahn, J.; Bromke, M.; Vera-Villalobos, H.; Li, Y.; Frenzel, F.; Giavalisco, P.; Ribera-Fonseca, A.; Zunino, L.; et al. Sulphate Fertilization Ameliorates Long-Term Aluminum Toxicity Symptoms in Perennial Ryegrass (*Lolium perenne*). *Plant Physiol. Biochem.* **2014**, *83*, 88–99. [CrossRef]

19. Reyes-Díaz, M.; Inostroza-Blancheteau, C.; Millaleo, R.; Cruces, E.; Wulff-Zottele, C.; Alberdi, M.; de la Luz Mora, M. Long-Term Aluminum Exposure Effects on Physiological and Biochemical Features of Highbush Blueberry Cultivars. *J. Am. Soc. Hortic. Sci.* **2010**, *135*, 212–222. [CrossRef]
20. Reyes-Diaz, M.; Alberdi, M.; Mora, M.D.L.L. Short-Term Aluminum Stress Differentially Affects the Photochemical Efficiency of Photosystem II in Highbush Blueberry Genotypes. *J. Am. Soc. Hortic. Sci.* **2009**, *134*, 14–21. [CrossRef]
21. Cheng, X.; Fang, T.; Zhao, E.; Zheng, B.; Huang, B.; An, Y.; Zhou, P. Protective Roles of Salicylic Acid in Maintaining Integrity and Functions of Photosynthetic Photosystems for Alfalfa (*Medicago sativa* L.) Tolerance to Aluminum Toxicity. *Plant Physiol. Biochem.* **2020**, *155*, 570–578. [CrossRef]
22. Phukunkamkaew, S.; Tisarum, R.; Pipatsitee, P.; Samphumphuang, T.; Maksup, S.; Cha-um, S. Morpho-Physiological Responses of Indica Rice (*Oryza sativa* Sub. indica) to Aluminum Toxicity at Seedling Stage. *Environ. Sci. Pollut. Res.* **2021**, *28*, 29321–29331. [CrossRef]
23. Ofoe, R.; Thomas, R.H.; Asiedu, S.K.; Wang-Pruski, G.; Fofana, B.; Abbey, L. Aluminum in Plant: Benefits, Toxicity and Tolerance Mechanisms. *Front. Plant Sci.* **2023**, *13*, 1085998. [CrossRef] [PubMed]
24. Guo, P.; Li, Q.; Qi, Y.P.; Yang, L.T.; Ye, X.; Chen, H.H.; Chen, L.S. Sulfur-Mediated-Alleviation of Aluminum-Toxicity in Citrus Grandis Seedlings. *Int. J. Mol. Sci.* **2017**, *18*, 2570. [CrossRef] [PubMed]
25. Ritchey, K.D.; Snuffer, J.D. Limestone, Gypsum, and Magnesium Oxide Influence Restoration of an Abandoned Appalachian Pasture. *Agron. J.* **2002**, *94*, 830–839. [CrossRef]
26. Demanet-Fillipi, R. Enmiendas Calcareas. Plant Lechero Watt´s. Chile. Bulletin N°2. April 2017. Available online: https://www.watts.cl/docs/default-source/charlas-a-productores/enmienda-calcarea.pdf?sfvrsn=4 (accessed on 30 October 2023).
27. Meriño-Gergichevich, C.; Alberdi, M.; Ivanov, A.G.; Reyes-Díaz, M. Al^{3+}-Ca^{2+} Interaction in Plants Growing in Acid Soils: Al-Phytotoxicity Response to Calcareous Amendments. *J. Soil Sci. Plant Nutr.* **2010**, *10*, 217–243.
28. Toma, M.; Sumner, M.E.; Weeks, G.; Saigusa, M. Long-term Effects of Gypsum on Crop Yield and Subsoil Chemical Properties. *Soil Sci. Soc. Am. J.* **1999**, *63*, 891–895. [CrossRef]
29. Takahashi, T.; Ikeda, Y.; Nakamura, H.; Nanzyo, M. Efficiency of Gypsum Application to Acid Andosols Estimated Using Aluminum Release Rates and Plant Root Growth. *Soil Sci. Plant Nutr.* **2006**, *52*, 584–592. [CrossRef]
30. Kinraide, T.B. Identity of the Rhizotoxic Aluminium Species. *Plant Soil* **1991**, *134*, 167–178. [CrossRef]
31. Mora, M.L.; Cartes, P.; Demanet, R.; Cornforth, I.S. Effects of Lime and Gypsum on Pasture Growth and Composition on an Acid Andisol in Chile, South America. *Commun. Soil Sci. Plant Anal.* **2002**, *33*, 2069–2081. [CrossRef]
32. Vera-Villalobos, H.; Lunario-Delgado, L.; Pérez-Retamal, D.; Román, D.; Leiva, J.C.; Zamorano, P.; Mercado-Seguel, A.; Gálvez, A.S.; Benito, C.; Wulff-Zottele, C. Sulfate Nutrition Improves Short-Term Al3+-Stress Tolerance in Roots of *Lolium perenne* L. *Plant Physiol. Biochem.* **2020**, *148*, 103–113. [CrossRef] [PubMed]
33. Takahashi, H.; Kopriva, S.; Giordano, M.; Saito, K.; Hell, R. Sulfur Assimilation in Photosynthetic Organisms: Molecular Functions and Regulations of Transporters and Assimilatory Enzymes. *Annu. Rev. Plant Biol.* **2011**, *62*, 157–184. [CrossRef]
34. Saito, K. Sulfur Assimilatory Metabolism. The Long and Smelling Road. *Plant Physiol.* **2004**, *136*, 2443–2450. [CrossRef] [PubMed]
35. Zhu, C.Q.; Zhang, J.H.; Sun, L.M.; Zhu, L.F.; Abliz, B.; Hu, W.J.; Zhong, C.; Bai, Z.G.; Sajid, H.; Cao, X.C.; et al. Hydrogen Sulfide Alleviates Aluminum Toxicity via Decreasing Apoplast and Symplast al Contents in Rice. *Front. Plant Sci.* **2018**, *9*, 294. [CrossRef]
36. Alarcón-Poblete, E.; Inostroza-Blancheteau, C.; Alberdi, M.; Rengel, Z.; Reyes-Díaz, M. Molecular Regulation of Aluminum Resistance and Sulfur Nutrition during Root Growth. *Planta* **2018**, *247*, 27–39. [CrossRef] [PubMed]
37. Taylor, G.J.; Foy, C.D. Mechanisms of Aluminum Tolerance in *Triticum aestivum* L. (Wheat). I. Differential PH Induced by Winter Cultivars in Nutrient Solutions. *Am. J. Bot.* **1985**, *72*, 695–701. [CrossRef]
38. Shaff, J.E.; Schultz, B.A.; Craft, E.J.; Clark, R.T.; Kochian, L.V. GEOCHEM-EZ: A Chemical Speciation Program with Greater Power and Flexibility. *Plant Soil* **2010**, *330*, 207–214. [CrossRef]
39. Román-Silva, D.A.; Rivera, L.; Morales, T.; Ávila, J.; Cortés, P. Determination of Trace Elements in Environmental and Biological Samples Using Improved Sample Introduction in Flame Atomic Absorption Spectrometry (HHPN-AAS; HHPN-FF-AAS). *Int. J. Environ. Anal. Chem.* **2003**, *83*, 327–341. [CrossRef]
40. Du, Z.; Bramlage, W.J. Modified Thiobarbituric Acid Assay for Measuring Lipid Oxidation in Sugar-Rich Plant Tissue Extracts. *J. Agric. Food Chem.* **1992**, *40*, 1566–1570. [CrossRef]
41. Gillespie, K.M.; Ainsworth, E.A. Measurement of Reduced, Oxidized and Total Ascorbate Content in Plants. *Nat. Protoc.* **2007**, *2*, 871–874. [CrossRef]
42. Rahman, I.; Kode, A.; Biswas, S.K. Assay for Quantitative Determination of Glutathione and Glutathione Disulfide Levels Using Enzymatic Recycling Method. *Nat. Protoc.* **2007**, *1*, 3159–3165. [CrossRef] [PubMed]
43. Donahue, J.L.; Okpodu, C.M.; Cramer, C.L.; Grabau, E.A.; Alscher, R.G. Responses of Antioxidants to Paraquat in Pea Leaves: Relationships to Resistance. *Plant Physiol.* **1997**, *113*, 249–257. [CrossRef]
44. Nakano, Y.; Asada, K. Hydrogen Peroxide Is Scavenged by Ascorbate-Specific Peroxidase in Spinach Chloroplasts. *Plant Cell Physiol.* **1981**, *22*, 867–880. [CrossRef]
45. Ambuko, J.; Carmel Zanol, G.; Sekozawa, Y.; Sugaya, S.; Gemma, H. Reactive Oxygen Species (ROS) Scavenging in Hot Air Preconditioning Mediated Alleviation of Chilling Injury in Banana Fruits. *J. Agric. Sci.* **2012**, *5*, 319. [CrossRef]
46. Aebi, H. [13] Catalase in vitro. *Methods Enzymol.* **1984**, *105*, 121–126. [CrossRef] [PubMed]

47. Untergasser, A.; Ruijter, J.M.; Benes, V.; van den Hoff, M.J.B. Web-Based LinRegPCR: Application for the Visualization and Analysis of (RT)-QPCR Amplification and Melting Data. *BMC Bioinform.* **2021**, *22*, 398. [CrossRef]
48. Schmittgen, T.D.; Livak, K.J. Analysis of Relative Gene Expression Data Using Real-Time Quantitative PCR and the $2^{-\Delta\Delta CT}$ Method. *Methods* **2001**, *25*, 402–408.
49. Chen, W.W.; Tang, L.; Wang, J.Y.; Zhu, H.H.; Jin, J.F.; Yang, J.L.; Fan, W. Research Advances in the Mutual Mechanisms Regulating Response of Plant Roots to Phosphate Deficiency and Aluminum Toxicity. *Int. J. Mol. Sci.* **2022**, *23*, 1137. [CrossRef]
50. Correia, S.; Matos, M.; Ferreira, V.; Martins, N.; Gonçalves, S.; Romano, A.; Pinto-Carnide, O. Molecular Instability Induced by Aluminum Stress in Plantago Species. *Mutat. Res./Genet. Toxicol. Environ. Mutagen.* **2014**, *770*, 105–111. [CrossRef]
51. Yang, M.; Tan, L.; Xu, Y.; Zhao, Y.; Cheng, F.; Ye, S.; Jiang, W. Effect of Low PH and Aluminum Toxicity on the Photosynthetic Characteristics of Different Fast-Growing Eucalyptus Vegetatively Propagated Clones. *PLoS ONE* **2015**, *10*, e0130963. [CrossRef]
52. Lyčka, M.; Barták, M.; Helia, O.; Kopriva, S.; Moravcová, D.; Hájek, J.; Fojt, L.; Čmelík, R.; Fajkus, J.; Fojtová, M. Sulfate supplementation affects nutrient and photosynthetic status of Arabidopsis thaliana and Nicotiana tabacum differently under prolonged exposure to cadmium. *J. Hazard. Mater.* **2023**, *445*, 130527. [CrossRef]
53. Narayan, O.P.; Kumar, P.; Yadav, B.; Dua, M.; Johri, A.K. Sulfur nutrition and its role in plant growth and development. *Plant Signal. Behav.* **2022**, *9*, 2030082. [CrossRef] [PubMed]
54. Chen, J.; Duan, R.X.; Hu, W.J.; Zhang, N.N.; Lin, X.Y.; Zhang, J.H.; Zheng, H.L. Unravelling Calcium-Alleviated Aluminium Toxicity in Arabidopsis Thaliana: Insights into Regulatory Mechanisms Using Proteomics. *J. Proteom.* **2019**, *199*, 15–30. [CrossRef] [PubMed]
55. Mariano, E.D.; Keltjens, W.G. Long-Term Effects of Aluminum Exposure on Nutrient Uptake by Maize Genotypes Differing in Aluminum Resistance. *J. Plant Nutr.* **2005**, *28*, 323–333. [CrossRef]
56. Danyaei, A.; Hassanpour, S.; Baghaee, M.A.; Dabbagh, M.; Babarabie, M. The Effect of Sulfur-Containing Humic Acid on Yield and Nutrient Uptake in Olive Fruit. *Open J. Ecol.* **2017**, *7*, 279–288. [CrossRef]
57. Salvagiotti, F.; Castellarín, J.M.; Miralles, D.J.; Pedrol, H.M. Sulfur Fertilization Improves Nitrogen Use Efficiency in Wheat by Increasing Nitrogen Uptake. *Field Crops Res.* **2009**, *113*, 170–177. [CrossRef]
58. Shafiq, B.A.; Nawaz, F.; Majeed, S.; Aurangzaib, M.; Al Mamun, A.; Ahsan, M.; Ahmad, K.S.; Shehzad, M.A.; Ali, M.; Hashim, S.; et al. Sulfate-Based Fertilizers Regulate Nutrient Uptake, Potosynthetic Gas Exchange, and Enzymatic Antioxidants to Increase Sunflower Growth and Yield Under Drought Stress. *J. Soil Sci. Plant Nutr.* **2021**, *21*, 2229–2241. [CrossRef]
59. Mariño Macana, Y.A.; de Toledo, F.H.S.F.; de Vicente Ferraz, A.; de Moraes Gonçalves, J.L.; Díaz López, S.M.; Barrero Cubillos, C.A.; Sierra Rojas, Á.N.; Bolognani, H.A. Soil Fertility and Fine Root Distribution after Gypsum Application in Eucalyptus Plantations with Different Tolerance to Water Deficit. *New For.* **2020**, *51*, 1039–1054. [CrossRef]
60. Hussain, B.; Ma, Y.; Li, J.; Gao, J.; Ullah, A.; Tahir, N. Cadmium in Rice Is Affected by Fertilizer-Borne Chloride and Sulfate Anions: Long-Term Field Versus Pot Experiments. *Processes* **2022**, *10*, 1253. [CrossRef]
61. Yan, S.; Yang, J.; Si, Y.; Tang, X.; Ma, Y.; Ye, W. Arsenic and cadmium bioavailability to rice (*Oryza sativa* L.) plant in paddy soil: Influence of sulfate application. *Chemosphere* **2022**, *307*, 135641. [CrossRef]
62. Nagayama, T.; Nakamura, A.; Yamaji, N.; Satoh, S.; Furukawa, J.; Iwai, H. Changes in the Distribution of Pectin in Root Border Cells Under Aluminum Stress. *Front. Plant Sci.* **2019**, *10*, 1216. [CrossRef]
63. Yan, L.; Riaz, M.; Liu, J.; Liu, Y.; Zeng, Y.; Jiang, C. Boron Reduces Aluminum Deposition in Alkali-Soluble Pectin and Cytoplasm to Release Aluminum Toxicity. *J. Hazard. Mater.* **2021**, *401*, 123388. [CrossRef]
64. Jaskowiak, J.; Kwasniewska, J.; Milewska-Hendel, A.; Kurczynska, E.U.; Szurman-Zubrzycka, M.; Szarejko, I. Aluminum Alters the Histology and Pectin Cell Wall Composition of Barley Roots. *Int. J. Mol. Sci.* **2019**, *20*, 3039. [CrossRef]
65. Sato, M.; Nagano, M.; J In, S.; Miyagi, A.; Yamaguchi, M.; Kawai-Yamada, M.; Ishikawa, T. Plant-Unique Cis/Trans Isomerism of Long-Chain Base Unsaturation Is Selectively Required for Aluminum Tolerance Resulting from Glucosylceramide-Dependent Plasma Membrane Fluidity. *Plants* **2020**, *9*, 19. [CrossRef]
66. Kochian, L.V. Cellular Mechanisms of Aluminum Toxicity and Resistance in Plants. *Annu. Rev. Plant Physiol. Plant Mol. Biol.* **1995**, *46*, 237–260. [CrossRef]
67. Tanoi, K.; Kobayashi, N.I. Leaf Senescence by Magnesium Deficiency. *Plants* **2015**, *4*, 756–772. [CrossRef]
68. Filipovic, M.R.; Jovanović, V.M. More than Just an Intermediate: Hydrogen Sulfide Signalling in Plants. *J. Exp. Bot.* **2017**, *68*, 4733–4736. [CrossRef]
69. Silva, G.S.; Gavassi, M.A.; Nogueira, M.A.; Habermann, G. Aluminum Prevents Stomatal Conductance from Responding to Vapor Pressure Deficit in *Citrus limonia*. *Environ. Exp. Bot.* **2018**, *155*, 662–671. [CrossRef]
70. Kasajima, I. Difference in Oxidative Stress Tolerance between Rice Cultivars Estimated with Chlorophyll Fluorescence Analysis. *BMC Res. Notes* **2017**, *10*, 168. [CrossRef] [PubMed]
71. Maina, J.N.; Wang, Q. Seasonal Response of Chlorophyll a/b Ratio to Stress in a Typical Desert Species: Haloxylon Ammodendron. *Arid. Land Res. Manag.* **2015**, *29*, 321–334. [CrossRef]
72. Mathot, M.; Thélier-Huché, L.; Lambert, R. Sulphur and Nitrogen Content as Sulphur Deficiency Indicator for Grasses. *Eur. J. Agron.* **2009**, *30*, 172–176. [CrossRef]
73. Howarth, J.R.; Parmar, S.; Jones, J.; Shepherd, C.E.; Corol, D.I.; Galster, A.M.; Hawkins, N.D.; Miller, S.J.; Baker, J.M.; Verrier, P.J.; et al. Co-Ordinated Expression of Amino Acid Metabolism in Response to N and S Deficiency during Wheat Grain Filling. *J. Exp. Bot.* **2008**, *59*, 3675–3689. [CrossRef]

74. Alam, A.; Tariq, M.; Ali, J.; Adnan, M.; Fahad, S.; Ahmad, M.; Romman, M.; Saleem, M.H.; Okla, M.K.; Ahmad, S.; et al. Co-application of Phosphorus and Sulphur Improve Yield, Quality, and Nutrients Uptake in *Nicotiana tabaccum* L. *Philipp. Agric. Sci.* **2022**, *105*, 61–68. [CrossRef]
75. Mittler, R. Oxidative Stress, Antioxidants and Stress Tolerance. *Trends Plant Sci.* **2002**, *7*, 405–410. [CrossRef] [PubMed]
76. Sharma, P.; Jha, A.B.; Dubey, R.S.; Pessarakli, M. Reactive Oxygen Species, Oxidative Damage, and Antioxidative Defense Mechanism in Plants under Stressful Conditions. *J. Bot.* **2012**, *2012*, 217037. [CrossRef]
77. Mittler, R.; Vanderauwera, S.; Gollery, M.; Van Breusegem, F. Reactive Oxygen Gene Network of Plants. *Trends Plant Sci.* **2004**, *9*, 490–498. [CrossRef] [PubMed]
78. Lima-Melo, Y.; Alencar, V.T.C.B.; Lobo, A.K.M.; Sousa, R.H.V.; Tikkanen, M.; Aro, E.M.; Silveira, J.A.G.; Gollan, P.J. Photoinhibition of Photosystem i Provides Oxidative Protection during Imbalanced Photosynthetic Electron Transport in Arabidopsis Thaliana. *Front. Plant Sci.* **2019**, *10*, 916. [CrossRef] [PubMed]
79. Sachdev, S.; Ansari, S.A.; Ansari, M.I.; Fujita, M.; Hasanuzzaman, M. Abiotic Stress and Reactive Oxygen Species: Generation, Signaling, and Defense Mechanisms. *Antioxidants* **2021**, *10*, 277. [CrossRef]
80. Moustaka, J.; Ouzounidou, G.; Sperdouli, I.; Moustakas, M. Photosystem II Is More Sensitive than Photosystem I to Al^{3+} Induced Phytotoxicity. *Materials* **2018**, *11*, 1772. [CrossRef]
81. Zhu, D.B.; Hu, K.D.; Guo, X.K.; Liu, Y.; Hu, L.Y.; Li, Y.H.; Wang, S.H.; Zhang, H. Sulfur Dioxide Enhances Endogenous Hydrogen Sulfide Accumulation and Alleviates Oxidative Stress Induced by Aluminum Stress in Germinating Wheat Seeds. *Oxidative Med. Cell. Longev.* **2015**, *2015*, 612363. [CrossRef]